

Comparison of discovery limits for E_6 neutral gauge bosons at future colliders

Simon Capstick*

Department of Theoretical Physics, Oxford University, 1 Keble Road, Oxford OX1 3NP, United Kingdom

Stephen Godfrey*

Physics Department, Brookhaven National Laboratory, Upton, New York 11973

(Received 4 September 1987)

We study and compare the phenomenology of extra E_6 neutral gauge bosons at e^+e^- , ep , and hadron colliders. Our purpose is to compare the discovery reach of the various colliders and see how they compare in studying the phenomenology of extra neutral gauge bosons. We find that of the future colliders, hadron colliders probe the highest mass scales for the existence of extra neutral gauge bosons although precision measurements at e^+e^- colliders, the SLAC Linear Collider and CERN's LEP, at $\sqrt{s} = M_{Z^0}$ will put tight constraints on models predicting extra neutral gauge bosons. If deviations from the standard model are observed at e^+e^- colliders at $\sqrt{s} = M_{Z^0}$, other measurements, especially those at the DESY ep collider HERA, will be necessary to unravel the physics. We also find that high-precision, low-energy neutral-current experiments will be competitive with e^+e^- and ep colliders for detecting the presence of extra E_6 neutral gauge bosons.

I. INTRODUCTION

Despite agreement of the standard model with all existing data many puzzles remain such as the number of fermion generations and the large fermion mass differences. These questions, along with others, have led to the prejudice that the standard model is the low-energy limit of a more fundamental theory. There have been various speculations about what the larger theory could be, but one ingredient common to many of them is the prediction of extra neutral gauge bosons.¹⁻³ One such theory, grand unified theories based on the group E_6 , has attracted considerable attention because of its possible relevance as the low-energy limit of superstring theories.² Although we do not know if superstrings will turn out to be the "theory of everything," E_6 grand unified theories (GUT's) are very rich in new phenomenology and as such provide a framework to study new physics; in particular, they offer a convenient means of parametrizing extra neutral gauge bosons.

Considerable effort has been extended in studying the effects of extra E_6 neutral gauge bosons on a wide variety of measurements ranging from existing low-energy neutral-current measurements⁴⁻⁶ to future high-energy collider experiments.⁷⁻¹³ It was found that existing data allow for extra neutral gauge bosons (Z 's) with masses well below 1 TeV (Refs. 4-6). In this paper we examine the phenomenology of extra E_6 neutral gauge bosons at the future e^+e^- , ep , and hadron colliders whose parameters we summarize in Table I. Our aim is to compare the discovery reaches of these colliders and point out their strengths and weaknesses in studying the various properties of extra neutral gauge bosons. In one form or another many of the processes we consider have been studied elsewhere. However, in this paper we put these measurements, and several new ones, into a common format so

that the discovery limits of individual experiments can be compared and put into their proper perspective. Although we use the example of E_6 GUT's in our calculations our conclusions should be relevant to other models of interest which predict extra neutral gauge bosons due to the wide range of Z' -fermion couplings contained in E_6 . Hopefully the lessons we learn in this analysis will transcend the immediate motivation.

We begin in Sec. II with a brief overview of E_6 GUT's necessary to describe the parameters of extra neutral gauge bosons. In Sec. III we examine the constraints on extra neutral gauge bosons obtained from existing neutral-current data along with the expected discovery reach of future atomic parity and neutrino-electron cross-section measurements. We then proceed in Sec. IV to study the phenomenology of extra neutral gauge bosons at the e^+e^- colliders, KEK's TRISTAN, the SLAC Linear Collider (SLC), and CERN's LEP and LEP II; the ep collider, DESY's HERA; and the hadron colliders, Fermilab's Tevatron, Serpukhov's UNK collider, CERN's Large Hadron Collider (LHC), and the Superconducting Super Collider (SSC). Finally in Sec. V we summarize our results and state our conclusions.

II. E_6 CONSIDERATIONS

E_6 considerations have been discussed in detail elsewhere.^{5,7,14} In what follows we give a cursory review to define our notation and the parameters of the model, in particular, the couplings of fermions to the extra Z^0 boson, and refer the interested reader to more detailed discussions in the literature. Since E_6 is a rank-6 group it has six diagonal generators. Two are accounted for by $SU(3)_C$ and one each by the electromagnetic and Z^0 charge generators leaving two available for new physics and hence extra neutral gauge bosons. Since the $U(1)$

TABLE I. Expected machine parameters of future high-energy colliders [Particle Data Group, Phys. Lett. 170B, 1 (1986)].

Collider	Particles collided	\sqrt{s} (Gev)	Luminosity ($\text{cm}^{-2}\text{s}^{-1}$)	Integrated luminosity ^a (pb^{-1})
TRISTAN	e^+e^-	60	2×10^{31}	2×10^2
SLC	e^+e^-	100	6×10^{30}	6×10
LEP	e^+e^-	120	1.6×10^{31}	1.6×10^2
LEP II	e^+e^-	200	1.6×10^{31}	1.6×10^2
HERA	ep	314	1.5×10^{31}	1.5×10^2
		253	9.0×10^{31}	9.0×10^2
Tevatron	$p\bar{p}$	1.8×10^3	10^{30}	10
UNK	pp	6×10^3	10^{32}	10^3
LHC	pp	17×10^3	10^{33}	10^4
SSC	pp	40×10^3	10^{33}	10^4

^aFor 10^7 -sec year of running.

generator of the extra neutral gauge boson must be orthogonal to the generators of the standard model it is convenient to label it in terms of the subgroup chain,

$$E_6 \rightarrow \text{SO}(10) \times \text{U}(1)_\psi \rightarrow \text{SU}(5) \times \text{U}(1)_\chi \times \text{U}(1)_\psi, \quad (1)$$

where the $\text{SU}(3)_C \times \text{SU}(2)_L \times \text{U}(1)_{Y_W}$ group of the standard model is embedded in the $\text{SU}(5)$ subgroup. Thus, depending on the specific model and its symmetry breakdown, the Z' charges will be given by a linear combination of the $\text{U}(1)_\chi$ and $\text{U}(1)_\psi$ charges:

$$Q_{E_6} = Q_\chi \cos\theta_{E_6} + Q_\psi \sin\theta_{E_6}, \quad (2)$$

where Q_χ and Q_ψ are given in Table II and the mixing angle θ_{E_6} is determined by the specific E_6 model. We have implicitly assumed that if there are two extra neutral gauge bosons one will be sufficiently heavy so as not to be relevant to the present analysis. In this notation $\theta_{E_6} = \theta_\chi = 0$ corresponds to the extra Z^0 of $\text{SO}(10)$, $\theta_{E_6} = \theta_\psi = 90^\circ$ to the extra Z^0 of E_6 , and $\theta_{E_6} = \theta_\eta = \arctan(-\sqrt{5/3}) \simeq -52^\circ$ to the extra Z^0 popular in some superstring theories.²

That E_6 includes a large range of couplings is illustrated in Fig. 1 where we have plotted the Z_{E_6} -fermion cou-

TABLE II. Extra- E_6 -neutral-gauge-boson charges of the first-generation fermions. The charge of the right-handed components Q_{f_R} are equal to $-Q_{f_L^c}$. The second- and third-generation fermions have the same charges as the corresponding first-generation fermions. N is the right-handed neutrino in $\text{SO}(10)$, h is a charge $-\frac{1}{3}$ isosinglet quark, (ν_E, E^-) is a lepton isodoublet, and n is a neutral isosinglet lepton.

	$2\sqrt{10}Q_\chi$	$2\sqrt{6}Q_\psi$	$2\sqrt{15}Q_\eta$
u, d, u^c, e^c	-1	1	-2
d^c, ν, e^-	3	1	1
N^c	-5	1	-5
h, N_E^c, E^c	2	-2	4
h^c, ν_E, E^-	-2	-2	1
n	0	4	-5

plings as a function of θ_{E_6} . For instance at $\theta_{E_6} = 90^\circ$ the electron and up quark's left- and right-handed couplings are equal and opposite, leading to purely axial-vector coupling to the extra-neutral gauge boson. At $\theta_{E_6} = \arctan(-\sqrt{27/5})$ Z_{E_6} decouples from ν_e . At $\theta_{E_6} = \arctan\sqrt{3/5}$ the u quark decouples from the Z' making the Z' harder to produce in hadron collisions. Although the parameter space covered is not exhaustive in the sense that it does not cover all the possibilities that would be available if we let the couplings vary independently, it does include a large range of possible couplings.

In general, the physical fields Z^0 and Z' are linear combinations of the gauge fields Z_{SM} and Z_{E_6} , with mixing angle ϕ . The mixing will alter the fermion couplings

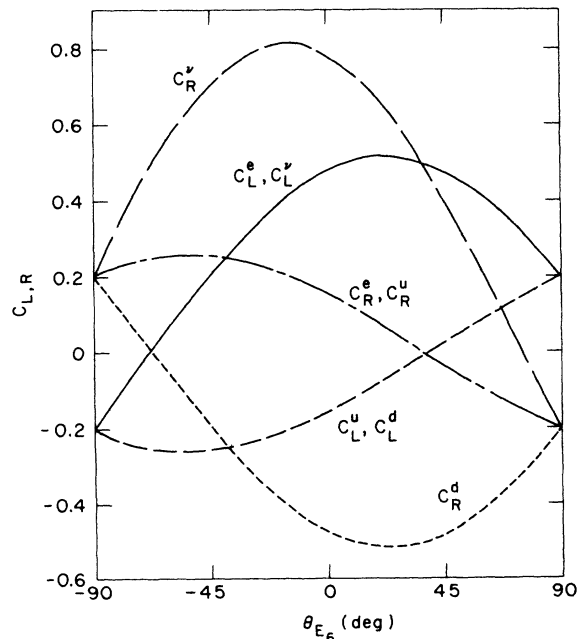


FIG. 1. Left- and right-handed-fermion- Z_{E_6} couplings as a function of θ_{E_6} . The couplings were obtained by substituting the charges in Table II into Eq. (2). Note that $C_R^f = -C_L^{f^c}$.

so that the physical fields' charges are given by a linear combination of the unmixed fields' charges:

$$C_{L,R} = C_{L,R}^{\text{SM}} \cos\phi + (g_{Z'}/g_{Z^0}) C_{L,R}^{E_6} \sin\phi, \quad (3a)$$

$$C'_{L,R} = -(g_{Z^0}/g_{Z'}) C_{L,R}^{\text{SM}} \sin\phi + C_{L,R}^{E_6} \cos\phi, \quad (3b)$$

where $C_{L,R}$ are the standard model Z^0 fermion charges given as usual by $C_{L,R} = I_{3L} - Q_{em} \sin^2\theta_W$ and $(g_{Z'}/g_{Z^0})$ is the ratio of the $U(1)_{E_6}$ coupling strength to the $U(1)_{Y_W}$ coupling strength. One finds from renormalization-group arguments that $(g_{Z'}/g_{Z^0})^2 \leq \frac{5}{3} \sin^2\theta_W$ with the exact value dependent on the specific symmetry-breaking scheme.³ Here we assume the equality which results when all $U(1)$ groups are broken at the same mass. For models in which the neutral gauge bosons acquire mass only via Higgs singlets or doublets, such as in superstring theories, ϕ is related to M_{Z^0} and $M_{Z'}$ by¹⁵

$$\tan^2\phi = \frac{M_{\text{SM}}^2 - M_{Z^0}^2}{M_{Z'}^2 - M_{\text{SM}}^2}, \quad (4)$$

where $M_{\text{SM}} = M_W / \cos\theta_W$. Thus, precision measurements of ϕ along with measurements of M_{Z^0} , $\sin^2\theta_W$, and M_W can set limits on the Z' mass in these models.

The neutral-current Lagrangian for the extended model is

$$-L_{\text{NC}} = e A_\mu J_{\text{em}}^\mu + g_{Z^0} Z_\mu^0 J_{Z^0}^\mu + g_{Z'} Z'_\mu J_{Z'}^\mu, \quad (5)$$

where J_{em}^μ is the usual electromagnetic current, $J_{Z^0}^\mu = \sum_f C_L^f \bar{f}_L \gamma^\mu f_L$, and $J_{Z'}^\mu = \sum_f C_L^f \bar{f}_L \gamma^\mu f_L$ with the sum over left-handed fermion fields. Thus, for a given θ_{E_6} we are left with $M_{Z'}$ and ϕ as unknown quantities. In general the discovery limits for $M_{Z'}$ are two-dimensional surfaces which are functions of both θ_{E_6} and ϕ . To simplify the analysis we consider two slices in parameter space; $M_{Z'}$ vs ϕ for the case of θ_η and $M_{Z'}$ vs θ_{E_6} with $\phi=0$. In the first case we will find that high-precision measurements in e^+e^- collisions at $\sqrt{s} = M_{Z^0}$ will probe very small values of ϕ (Refs. 7–9). If deviations from the standard model are not observed, the resulting limits on ϕ will be such that bounds obtained on $M_{Z'}$ from other experiments will not differ significantly from the bounds obtained for $\phi=0$.

III. EXISTING BOUNDS AND FUTURE LOW-ENERGY NEUTRAL-CURRENT MEASUREMENTS

Before proceeding to future colliders we first consider the bounds which existing neutral-current data put on $M_{Z'}$ and ϕ to give a benchmark against which to measure future experiments. In Fig. 2 the solid line gives the 95%-confidence-level lower bounds on $M_{Z'}$ as a function of θ_{E_6} for $\phi=0$ (Ref. 16). To obtain this curve we follow the analysis of London and Rosner (Ref. 5) with two changes: We use $M_{Z^0} = 92.3 \pm 1.7$ GeV, $M_W = 80.8 \pm 1.4$ GeV (Ref. 17), and for the weak charge in atomic parity violation in cesium we use the experimental value¹⁸ of

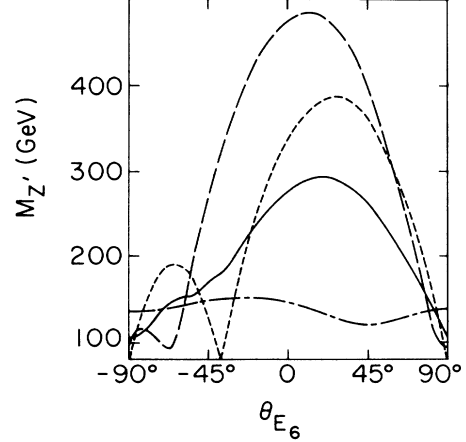


FIG. 2. Existing bounds and future discovery limits of extra E_6 neutral gauge bosons as a function of θ_{E_6} for $\phi=0$. The solid line gives the existing bound from neutral-current measurements. The short-dashed-long-dashed line gives the limit from combined UA1-UA2 data for Drell-Yan production of extra neutral gauge bosons. The short-dashed line gives the bounds obtainable from atomic parity measurement of $Q_W(\text{Cs})$ to ± 3 . The long-dashed line gives the bound obtainable by measuring $R = \sigma(\nu_\mu e^-) / \sigma(\bar{\nu}_\mu e^-)$ to an accuracy of 2%.

$Q_W(\text{Cs}) = -71.7 \pm 5.8$ which we compare to the radiatively corrected standard-model value of $-(22.5 \pm 216 \sin^2\theta_W)$ (Ref. 19). In comparison, the short-dashed-long-dashed curve in Fig. 2 gives the 95%-confidence-level (C.L.) lower limit on $M_{Z'}$ obtained by the combined UA1 + UA2 bound of $\sigma(p\bar{p} \rightarrow Z' \rightarrow e^+e^-) \leq 3$ pb at the CERN $S\bar{p}p$ S collider.¹⁷

Improvements in precision measurements of low-energy neutral-current processes will also add to our knowledge of extra neutral gauge bosons. Two such measurements are electron-neutrino scattering and atomic parity violation in cesium. For the case of electron-neutrino scattering, the cross sections are given by

$$\sigma(\nu_\mu e^- \rightarrow \nu_\mu e^-) = \frac{2G_\mu^2 m_e E_\nu}{\pi} (\epsilon_-^2 + \frac{1}{3}\epsilon_+^2), \quad (6a)$$

$$\sigma(\bar{\nu}_\mu e^- \rightarrow \bar{\nu}_\mu e^-) = \frac{2G_\mu^2 m_e E_\nu}{\pi} (\frac{1}{3}\epsilon_-^2 + \epsilon_+^2), \quad (6b)$$

where $G_\mu = g^2 / 4\sqrt{2} M_W^2 = 1.16636 \times 10^{-5} \text{ GeV}^{-2}$ and

$$\epsilon_- = \frac{1}{2}(1 - 2\sin^2\theta_W) - 2 \left[\frac{g_{Z'}}{g_{Z^0}} \right]^2 \left[\frac{M_{Z^0}}{M_{Z'}} \right]^2 C_L^{\nu\mu'} C_L^{e'}, \quad (7a)$$

$$\epsilon_+ = -\sin^2\theta_W - 2 \left[\frac{g_{Z'}}{g_{Z^0}} \right]^2 \left[\frac{M_{Z^0}}{M_{Z'}} \right]^2 C_L^{\mu\nu'} C_R^{e'}. \quad (7b)$$

For $\nu_e e^-$ and $\bar{\nu}_e e^-$ scattering ϵ_- is replaced by $(\epsilon_- - 1)$. A proposed 2% measurement at Los Alamos²⁰ of $\sigma(e^- \nu_\mu) / \sigma(e^- \bar{\nu}_\mu)$ gives the 95%-confidence-level bounds shown in Fig. 2 as the long-dashed lines.²¹

Similarly, precision measurements of atomic parity

violation in cesium are expected to measure the weak charge, $Q_W(\text{Cs})$ to ± 3 (Ref. 22). [It is worthwhile to note that the error is due not to experimental uncertainty but rather theoretical uncertainty of atomic physics effects in calculating $Q_W(\text{Cs})$.] This yields the 95%-C.L. bounds on $M_{Z'}$ given by the short-dashed lines in Fig. 2 where we have followed the analysis of Ref. 5 to obtain this curve.

IV. THE DISCOVERY REACH OF FUTURE COLLIDERS

We now turn to the discovery reach of the new and future high-energy colliders whose parameters are given in Table I.²³ In all cases, unless otherwise noted, we will base our discovery limits on the criterion that the effect of an extra neutral gauge boson must lie outside the 95% confidence limit of the standard model, based on the statistics one would expect from the standard model using the luminosities given in Table I and a standard 10^7 -sec year of running. For illustrative purposes we take for the standard-model parameters $M_{Z^0}=92.5$ GeV, $\Gamma_{Z^0}=2.5$ GeV, $\sin^2\theta_W=0.23$, and $\alpha_{em}^{-1}(M_W)=128.5$. We have not attempted to estimate systematic errors since they would be to a large extent detector dependent and although they would change the discovery limits the general comparison of different colliders should remain valid.

A. e^+e^- colliders

For e^+e^- collider measurements all results are derived from the differential cross section for a polarized e^- and an unpolarized e^+ (Ref. 7):

$$\frac{d\sigma(e^+e^- \rightarrow f\bar{f})}{d\cos\theta} = \frac{\pi\alpha^2}{4s} [|C_{LL}|^2(1+\cos\theta)^2 + |C_{LR}|^2(1-\cos\theta)^2], \quad (8)$$

where

$$C_{ij} = -Q_f + \frac{C_i^e C_j^f}{\sin^2\theta_W \cos^2\theta_W} \left[\frac{s}{s - M_{Z^0}^2 + i\Gamma_{Z^0} M_{Z^0}} \right] + \frac{(g_{Z'} / g_{Z^0})^2 C_i^{e'} C_j^{f'}}{\sin^2\theta_W \cos^2\theta_W} \left[\frac{s}{s - M_{Z'}^2 + i\Gamma_{Z'} M_{Z'}} \right]. \quad (9)$$

For right-handed electrons make the substitutions $C_{LL} \rightarrow C_{RR}$ and $C_{LR} \rightarrow C_{RL}$.

In the near future the most precise tests of the standard model will be precision measurements at $\sqrt{s} = M_{Z^0}$ at SLC and LEP. For the purpose of looking for Z^0 - Z' mixing the best measurements will be the longitudinal asymmetry²⁴ A_{LR} defined by

$$A_{LR} = \frac{\sigma(e_L^-) - \sigma(e_R^-)}{\sigma(e_L^-) + \sigma(e_R^-)}, \quad (10)$$

where the cross sections are obtained by integrating Eq. (8) over $\cos\theta$. At $\sqrt{s} = M_{Z^0}$ the cross section is dominated by the Z^0 pole so A_{LR} is given by

$$A_{LR} = \frac{|C_{LL}|^2 - |C_{RR}|^2}{|C_{LL}|^2 + |C_{RR}|^2 + 2|C_{LR}|^2} \simeq \frac{2C_V^e C_A^e}{C_V^{e2} + C_A^{e2}}, \quad (11)$$

where $C_{V,A} = \frac{1}{2}(C_L \pm C_R)$. (For electron polarization less than 100% the asymmetry is given by $A_{LR}^P = P A_{LR}^{P=1}$.^{8,9,24,25}) Thus, from Eq. (3) one sees that precision asymmetry measurements of the standard-model couplings will probe very small values of ϕ . For the process $\sigma(e^+e^- \rightarrow \mu^+\mu^-)$ with an integrated luminosity of 60 pb^{-1} , corresponding to a 10^7 sec year of running at the SLC design luminosity, and 100% polarization, the statistical uncertainty is $\delta A_{LR} \simeq 3 \times 10^{-3}$. (This corresponds to about $3.5 \times 10^6 Z^0$'s.) For θ_η , the superstring-inspired model, this results in the 95%-C.L. upper bound on ϕ given in Fig. 3 the by the short-dashed-long-dashed lines. More realistically, in the foreseeable future, the expected polarization at SLC will be approximately 45% with an uncertainty of $\Delta P/P \simeq 5\%$ (Ref. 24). This results in a measurement of A_{LR} at SLC to about 1%, and consequently, about a factor of 3 decrease in the bound on ϕ . For comparison, the existing bound from low-energy neutral-current data, taken from the analysis of Amaldi *et al.* (Ref. 4), is given by the solid curve in Fig. 3.

In addition to the above measurements, the polarization-asymmetry measurement, $A_{LR}(e^+e^-$

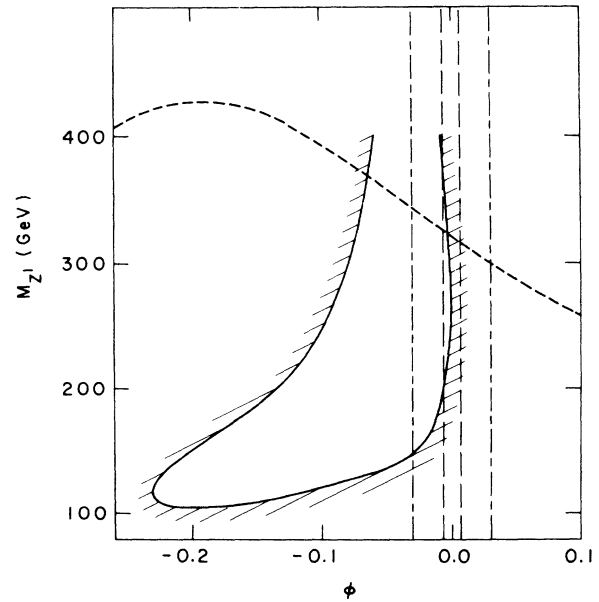


FIG. 3. Existing bounds and future discovery limits of Z_η as a function of ϕ . The solid line bounds the region ruled out at the 90% C.L. from existing neutral-current data as obtained by Amaldi *et al.* (Ref. 4). The short-dashed-long-dashed line gives the bounds obtained by measuring $A_{LR}(e^+e^- \rightarrow \mu^+\mu^-)$ at $\sqrt{s} = M_{Z^0}$ to 3×10^{-3} . The long-dashed line gives the bound obtainable by measuring $A_{LR}(e^+e^- \rightarrow \text{hadrons})$ at $\sqrt{s} = M_{Z^0}$ to 6×10^{-4} and the short-dashed line corresponds to bounds from measurements of the $\sigma(e_L^-) - \sigma(e_R^-)$ asymmetry in ep collisions at HERA at $\sqrt{s} = 253$ GeV with an integrated luminosity of $600 \text{ pb}^{-1}/\text{polarization}$.

→hadrons), is independent of the final-state fermions.²⁴ It has recently been shown by Lynn and Verzegnassi (Ref. 25) that this measurement is relatively insensitive to radiative corrections. Since the cross section to hadrons is much larger than to leptons this results in higher statistics and therefore more precise measurements of the Z^0 couplings. Using the same criteria as above results in a statistical error of $\delta A_{LR} \simeq 6 \times 10^{-4}$ which gives the 95%-C.L. upper bounds given by the long-dashed line in Fig. 3. Once again however, in the near future uncertainties in these measurements are likely to be about a factor of 3 larger with correspondingly weaker limits on ϕ . The higher statistics available at LEP give correspondingly better bounds, as the deviations in A_{LR} vary linearly with ϕ (Ref. 7). However, without polarized e^+ and e^- beams, LEP experiments will have to measure the polarization asymmetry by measuring τ lepton polarizations and it is not clear what sort of efficiencies they can achieve. For models where the gauge bosons acquire mass via Higgs singlets or doublets, as in superstring models, precision measurements of M_{Z^0} and ϕ combined with measurements of M_W and $\sin^2\theta_W$ would also give, using Eq. (4), a value for $M_{Z'}$.

Although precision measurements of A_{LR} can constrain ϕ for a given value of θ_{E_6} only one set of couplings, the electron couplings, are measured so θ_{E_6} cannot be determined without additional information. If deviations from the standard model are observed and are large enough one could use other measurements along with A_{LR} to extract the Z_{E_6} couplings to other fermions to determine θ_{E_6} (Refs. 7-9). For instance, if c and b quark flavor tagging is sufficiently efficient, one could measure $\Gamma(Z^0 \rightarrow c\bar{c})$, $\Gamma(Z^0 \rightarrow b\bar{b})$ and $A_{FB}(e^+e^- \rightarrow c\bar{c})$, $A_{FB}(e^+e^- \rightarrow b\bar{b})$, where

$$A_{FB} = \frac{\left[\int_0^1 - \int_{-1}^0 \right] d \cos\theta \frac{d\sigma}{d \cos\theta}}{\left[\int_0^1 + \int_{-1}^0 \right] d \cos\theta \frac{d\sigma}{d \cos\theta}} \simeq \frac{3}{4} A_{LR} \frac{2C_V^f C_A^f}{C_V^2 + C_A^2}. \quad (12)$$

However, since A_{FB} varies, roughly, quadratically with ϕ it is not clear if the latter measurements would be able to measure deviations from the standard model in A_{FB} .

Although these measurements at $\sqrt{s} = M_{Z^0}$ are fairly insensitive to the Z' mass they are by far the most restrictive measurements of Z^0 - Z' mixing. The bounds are so restrictive that if deviations from the standard model are

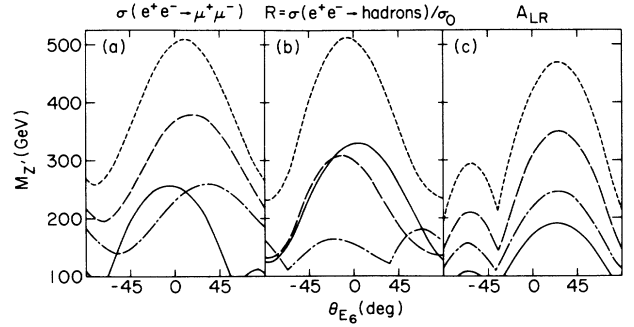


FIG. 4. Discovery limits for extra E_6 Z^0 's from e^+e^- measurements as a function of θ_{E_6} for $\phi=0$ using the center-of-mass energies and integrated luminosities given in Table I. The solid lines are for TRISTAN, the dotted-dashed lines are for SLC, the long-dashed lines for LEP, and the short-dashed lines for LEP II. In (a) the curves are for $\sigma(e^+e^- \rightarrow \mu^+\mu^-)$, in (b) for the hadron cross section $R = \sigma(e^+e^- \rightarrow \text{hadrons})/\sigma_0$, and in (c) for the longitudinal-polarization asymmetry (assuming 100% polarization).

not observed the allowed values of ϕ will be such that the bounds on $M_{Z'}$ obtained from other measurements will be essentially the same as those obtained by setting $\phi=0$. Thus, we will henceforth set $\phi=0$.

In addition to precision measurements at $\sqrt{s} = M_{Z^0}$ one can also obtain information about extra neutral gauge bosons at other center-of-mass energies.²⁶ These measurements would be especially important if Z^0 - Z' mixing turned out to be small. In Fig. 4 we show the discovery reach with $\phi=0$ for TRISTAN, SLC, LEP, and LEP II which could be obtained from measurements of $\sigma(e^+e^- \rightarrow \mu^+\mu^-)$, A_{LR} , and $\sigma(e^+e^- \rightarrow \text{hadrons})$ using the center-of-mass energies and integrated luminosities of Table I. These discovery limits, following our standard prescription, were obtained by requiring that the effect of an extra Z' lie outside the 95%-C.L. bound of the standard model. The standard-model predictions along with the 1σ statistical errors for these quantities are given in Table III. Although these limits result from complicated interference between the standard-model contributions and the E_6 contributions several features stand out. For instance, for A_{LR} , the low discovery reach at $\theta_{E_6} = -90^\circ$, 90° , and $\arctan(-\sqrt{3}/5) \simeq -38^\circ$ is a consequence of $C_L = \pm C_R$ resulting in either C_V^f or $C_A^f = 0$. For $\sigma(e^+e^- \rightarrow \mu^+\mu^-)$ and R the discovery limit is in general greatest at $\theta_{E_6} \simeq 0$. For \sqrt{s} sufficiently far away from the

TABLE III. The standard-model predictions and the 1σ statistical errors for $\sigma(e^+e^- \rightarrow \mu^+\mu^-)$, $R = \sigma(e^+e^- \rightarrow \text{hadrons})/\sigma_0$, and A_{LR} , where $\sigma_0 = 4\pi\alpha^2/3S$. The quantities were calculated using the center-of-mass energies in Table I and the statistical errors were estimated using the integrated luminosities given in Table I. The first column gives the numbers of events per year expected at each of the colliders.

Collider	σL	σ (pb)	$\delta\sigma$ (pb)	R	δR	A_{LR}	δA_{LR}
TRISTAN	5800	29	0.38	4.85	0.028	0.029	0.013
SLC	4100	68	1.1	12.4	0.045	0.19	0.016
LEP	1900	12	0.28	19.5	0.13	0.15	0.023
LEP II	480	3	0.14	8.0	0.14	0.086	0.046

Z^0 pole deviations from the standard model are dominated by Z^0 - Z' and γ - Z' interference which is proportional to $C_V^2 C_V'^2 + 2C_V C_A C_V' C_A' + C_A^2 C_A'^2$. Since for the photon $C_A = 0$, when C_V' is also equal to 0 deviations from the standard model become rather small.

$$\frac{d\sigma(e_L^- p)}{dx dy} = \frac{2\pi\alpha^2}{sx^2y^2} \sum_q \{x f_q(x, Q^2) [|b_{LL}|^2 + |b_{LR}|^2 (1-y)^2] + x f_{\bar{q}}(x, Q^2) [|b_{LR}|^2 + |b_{LL}|^2 (1-y)^2] \}, \quad (13)$$

where the sum runs over quark flavors. $f_q(x, Q^2)$ and $f_{\bar{q}}(x, Q^2)$ are the quark and antiquark distribution functions, $Q^2 = xys = -q^2$, and x and y are the usual scaling variables, $x = Q^2/2p \cdot q$, $y = p \cdot q/p \cdot k$.

$$b_{ij} = -Q_q + \frac{C_i^e C_j^q}{\sin^2\theta_w \cos^2\theta_w} \frac{Q^2}{Q^2 + M_{Z^0}^2} + \left[\frac{g_{Z'}}{g_{Z^0}} \right]^2 \frac{C_i^{e'} C_j^{q'}}{\sin^2\theta_w \cos^2\theta_w} \frac{Q^2}{Q^2 + M_{Z'}^2}, \quad (14)$$

where Q_q denotes the quark electric charge and $C_{L,R}$ and $C'_{L,R}$ are the left- and right-handed Z^0 and Z' charges given by (3a) and (3b). For the $e_L^+ p$ cross section make the substitutions $b_{LL} \rightarrow b_{RL}$ and $b_{LR} \rightarrow b_{RR}$, and to obtain the cross section for right-handed electrons and positrons make the substitution $L \leftrightarrow R$.

From the basic cross section one can make eight different measurements; the electron and positron cross sections $\sigma(e^-)$ and $\sigma(e^+)$, and the six asymmetries $e_L^- - e_R^-$, $e_L^- - e_R^+$, $e_R^- - e_L^+$, $e_L^+ - e_R^+$, $e_R^+ - e_L^-$, and $e_L^+ - e_R^-$, where the asymmetry $\alpha - \beta$ is defined by

$$A_{\alpha\beta} = [\sigma(\alpha) - \sigma(\beta)] / [\sigma(\alpha) + \sigma(\beta)].$$

In practice the most important facet of extending the reach in such measurements will be obtaining adequate statistics. Because the luminosity is expected to be approximately a factor of 6 higher²⁷ at $\sqrt{s} = 253$ GeV we have calculated the various asymmetries for this center-of-mass energy rather than at $\sqrt{s} = 314$ GeV, the maximum obtainable at HERA. In Fig. 3 the short-dashed curve gives the experimental reach for Z_η as a function of ϕ obtained from the $e_L^- - e_R^-$ asymmetry. Although this measurement is not as sensitive to ϕ as e^+e^- measurements it has the virtue of being sensitive to the Z' mass. Thus, if deviations from the standard model are observed at SLC or LEP, measurements at HERA could be crucial in understanding their origins. The discovery limits for several asymmetries with $\phi = 0$ are given in Fig. 5. To obtain these curves we use the Eichten-Hinchliffe-Lane-Quigg (EHLQ) structure functions²⁸ (set 2), integrated over the x and y variables from 0.1 to 1 and compared the E_6 results to those of the standard model.¹¹ The lower bound was so chosen because at small x the cross section is larger giving better statistics but with smaller deviations. At large x the deviations are larger but the statistics are poorer. Thus we take $x_{\min} = 0.1$ as a reasonable compromise which gives adequate statistics which are not

B. ep colliders

For ep collisions at HERA both left- and right-handed electrons and positrons can be collided with protons.²⁷ The differential cross section for ep collisions is given by

overwhelmed by the standard-model contributions. More sophisticated event binning would likely improve our bounds. Note that ep measurements are more sensitive to values of $\theta_{E_6} \simeq \pm 90^\circ$ than either low-energy neutral-current measurements or measurements at e^+e^- colliders. This is because in ep collisions the asymmetries are constructed using both $e_{L,R}^-$ and $e_{L,R}^+$ thereby measuring different combinations of couplings not available in e^+e^- colliders using only polarized electrons.

C. Hadron colliders

The Drell-Yan production of extra neutral gauge bosons in hadron colliders¹³ is very similar in form to Z' production in e^+e^- colliders except for the inclusion of the $q\bar{q}$ structure functions. Here the resonance cross section is given by

$$\frac{d\sigma(pp \rightarrow f\bar{f})}{dy} = \frac{x_A x_B \pi^2 \alpha_{em}^2 (g_{Z'}/g_{Z^0})^4}{9M_{Z'} \Gamma_{Z'}} (C_L^f{}^2 + C_R^f{}^2) \times \sum_q (C_L^{q^2} + C_R^{q^2}) G_q^+(x_A, x_B, Q^2), \quad (15)$$

where

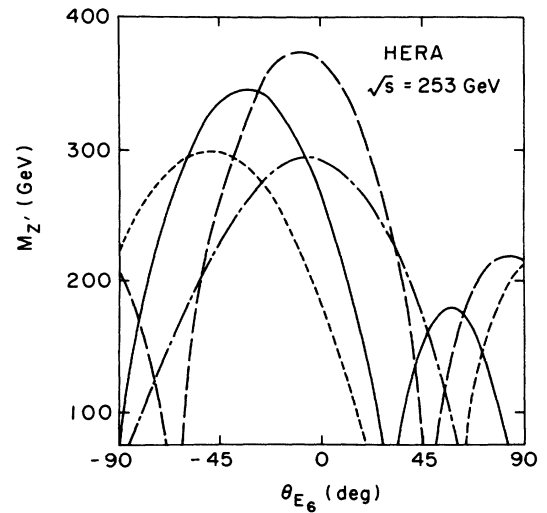


FIG. 5. Discovery limits for extra E_6 Z^0 s from ep measurements at HERA. All measurements are at $\sqrt{s} = 253$ GeV with an integrated luminosity of 600 pb^{-1} /polarization. The solid line is for the $e_L^- - e_R^-$ asymmetry, the long-dashed line is for the $e_L^- - e_R^+$ asymmetry, the short-dashed line is for the $e_R^- - e_L^+$ asymmetry, and the short-dashed-long-dashed line is for the $e_L^+ - e_R^+$ asymmetry.

$$G_q^+(x_A, x_B, Q^2) = \sum_q [f_{q/A}(x_A) f_{\bar{q}/B}(x_B) + f_{\bar{q}/A}(x_A) f_{q/B}(x_B)] . \quad (16)$$

The cross section for Z' production at hadron colliders is inversely proportional to the Z' width. Therefore, we must consider the effect of the extra fermions in E_6 on the Z' width. Since in E_6 the fundamental representation is a 27, for each generation there are 12 exotic fermion fields in addition to the 15 conventional ones.¹⁴ If exotic decay modes are kinematically allowed, the Z' width will become larger and more significantly the branching ratios to conventional fermions smaller. This is not important in e^+e^- and ep collisions since those processes proceed via virtual Z' 's in contrast with hadron colliders which rely on the Drell-Yan production of real Z' 's. Here we consider two cases: (1) no new decay modes are allowed and (2) the Z' can decay to 3 full generations of exotic fermions. The partial widths are given by

$$\Gamma_{Z' \rightarrow f\bar{f}} = M_{Z'} g_{Z'}^2 (C_{fL}^2 + C_{fR}^2) / 24\pi .$$

The discovery limits for hadron colliders,^{3,13,28} shown in Fig. 6, were obtained using the constraint that at least five $\mu^+\mu^-$ pairs will be produced for a given Z' mass where we used EHLQ structure functions²⁸ set 1 and the

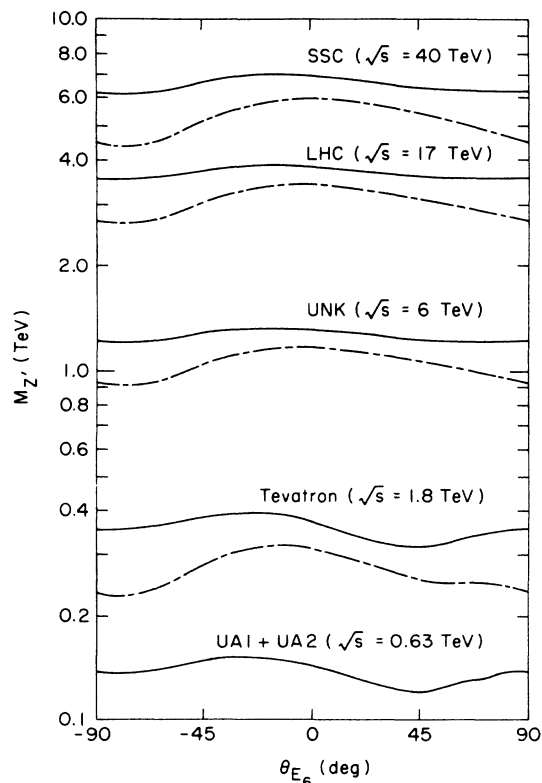


FIG. 6. Discovery limits for extra E_6 Z^0 's from hadron colliders. In all cases the solid lines represent the limits assuming that Z' decays to all exotic fermions are kinematically forbidden while the short-dashed-long-dashed lines represent the limits obtained assuming that the Z' can decay into three complete generations of exotics.

K factor given in Ref. 29. Lowering this constraint to three pairs per generation would raise the discovery reach about 10% while lowering the luminosity by a factor of 10 would reduce the reach by about a factor of 3. Note that higher mass scales could be probed for Z' 's if exotic decay modes with larger branching fractions are kinematically allowed.³⁰ We found that studying forward-backward asymmetries of lepton pairs would at best give discovery limits one-half as large as the direct production of lepton pairs. However, if an extra Z' was observed and it was low enough in mass to be produced in sufficient numbers it might be possible to determine its couplings and, hence θ_{E_6} , using forward-backward asymmetries.^{13,31}

V. SUMMARY AND CONCLUSIONS

Comparing the discovery reach of the various colliders and the two examples of low-energy experiments we found, to our surprise, that high-precision low-energy experiments do as well or better for many values of θ_{E_6} as the high-energy colliders that will become operational by about 1990. However, of all the measurements considered, hadron colliders were the least sensitive to θ_{E_6} and ϕ . To this we must comment on our criteria for the detection of extra Z^0 's. With the exception of hadron colliders we based our discovery limits on observing deviations from the standard model at the 95% confidence limit which corresponds to an effect of 1.64σ . This was reasonable for comparison purposes and may be valid for a global fit of many independent measurements but we doubt that such a deviation in one experiment would convince anybody that new physics has been discovered. In contrast the criteria we used in hadron colliders was for five dilepton events per generation leading to at least 10 clean dilepton events, possibly 15 if τ leptons could be reconstructed with reasonable efficiency. This would be fairly convincing evidence for a new particle. Our conclusion is that in the near future the Tevatron, assuming it reaches its design luminosity, will probe the highest mass scales for the existence of an extra E_6 neutral gauge boson. In the longer term, hadron colliders such as the SSC will be able to observe extra neutral gauge bosons provided they have masses less than about 6 TeV. Nevertheless, if a lower mass Z' were discovered, measurements by many experiments would be necessary to disentangle its properties.

ACKNOWLEDGMENTS

The authors are most grateful to Frank Paige and Bill Marciano for many helpful discussions and to Steve Barr and Sally Dawson for their encouragement in pursuing this analysis. S.C. wishes to thank the Natural Sciences and Engineering Research Council of Canada for their support. This work was supported by the U.S. Department of Energy under Contract No. DE-AC02-76CH00016 and the NSF through Grant No. 8116102.

- *Present address: Department of Physics, University of Guelph, Guelph, Canada N1G 2W1.
- ¹For recent reviews of composite vector bosons, see H. Harari, Report No. SLAC-PUB-4168 (unpublished); B. Schrempp, in *Proceedings of the XXIII International Conference on High Energy Physics*, Berkeley California, 1986, edited by S. Loken (World Scientific, Singapore, 1987).
- ²M. Green and J. Schwarz, Phys. Lett. **149B**, 117 (1984); **151B**, 21 (1985); D. Gross *et al.*, Phys. Rev. Lett. **54**, 502 (1985); E. Witten, Phys. Lett. **155B**, 1551 (1985); Nucl. Phys. **B258**, 75 (1985); P. Candelas *et al.*, *ibid.* **B258**, 46 (1985); M. Dine *et al.*, *ibid.* **B259**, 549 (1985); J. Ellis *et al.*, CERN Report No. CERN-TH-4350/86 1986 (unpublished); J. D. Breit, B. A. Ovrut, and G. C. Segrè, Phys. Lett. **158B**, 33 (1985); S. Cecotti *et al.*, *ibid.* **156B**, 318 (1985).
- ³R. W. Robinett, Phys. Rev. D **26**, 2388 (1982); R. W. Robinett and J. L. Rosner, *ibid.* **25**, 3036 (1982); **26**, 2396 (1982); P. Langacker, R. W. Robinett, and J. L. Rosner, *ibid.* **30**, 1470 (1984).
- ⁴U. Amaldi *et al.*, Phys. Rev. D **36**, 1385 (1987).
- ⁵D. London and J. Rosner, Phys. Rev. D **34**, 1530 (1986).
- ⁶L. S. Durkin and P. Langacker, Phys. Lett. **166B**, 436 (1986); V. Barger, N. G. Deshpande, and K. Whisnant, Phys. Rev. Lett. **56**, 30 (1986); S. M. Barr, *ibid.* **55**, 2778 (1985); E. Cohen *et al.*, Phys. Lett. **165B**, 76 (1985); W. J. Marciano and A. Sirlin, Phys. Rev. D **35**, 1672 (1987).
- ⁷G. Bélanger and S. Godfrey, Phys. Rev. D **34**, 1309 (1986); **35**, 378 (1987).
- ⁸P. J. Franzini and F. J. Gilman, Phys. Rev. D **35**, 855 (1987).
- ⁹M. Cvetič and B. Lynn, Phys. Rev. D **35**, 51 (1987).
- ¹⁰F. del Aguila, M. Quiros, and F. Zwirner, Nucl. Phys. **B284**, 530 (1987); I. Bigi and M. Cvetič, Phys. Rev. D **34**, 1651 (1986); T. Rizzo, *ibid.* **34**, 2699 (1986); C. Vaz and D. Wurmser, *ibid.* **33**, 2578 (1986); J. P. Ader, S. Narison, and J. C. Wallet, Phys. Lett. B **176**, 215 (1986); W. Hollik, Z. Phys. C **8**, 149 (1981); C. Dib and F. J. Gilman, Phys. Rev. D **36**, 1337 (1987).
- ¹¹S. Capstick and S. Godfrey, Phys. Rev. D **35**, 3351 (1987).
- ¹²V. D. Angelopoulos *et al.*, Phys. Lett. B **176**, 203 (1986); F. Cornet and R. Ruckl, *ibid.* **184**, 263 (1987).
- ¹³J. L. Rosner, Phys. Rev. D **35**, 2244 (1987); V. Barger *et al.*, *ibid.* **35**, 2893 (1987); F. del Aguila, M. Quiros, and F. Zwirner, Nucl. Phys. **B287**, 419 (1987); V. Barger, N. G. Deshpande, and K. Whisnant, Phys. Rev. D **35**, 1005 (1987).
- ¹⁴J. Rosner, Comments Nucl. Part. Phys. **15**, 195 (1986).
- ¹⁵P. Langacker, Phys. Rev. D **30**, 2008 (1984).
- ¹⁶A more rigorous analysis which includes more recent neutral-current data and radiative corrections give similar results. See Amaldi *et al.* (Ref. 4).
- ¹⁷S. Geer, in *Proceedings of the XXIII International Conference on High Energy Physics* (Ref. 1); A. Roussarie, *ibid.*
- ¹⁸C. Bouchiat and C. A. Piketty, Ecole Normale Supérieure report, 1986 (unpublished); M. A. Bouchiat, J. Guena, and L. Pottier, J. Phys. (Paris) **46**, 1897 (1985); S. Gilbert, M. Noecker, R. Watts, and C. Wieman, Phys. Rev. Lett. **55**, 2680 (1985).
- ¹⁹W. J. Marciano and A. Sirlin, Phys. Rev. D **27**, 552 (1983); **29**, 75 (1984).
- ²⁰D. H. White *et al.*, LAMPF Cherenkov Detector Proposal No. 1015, 1986 (unpublished).
- ²¹For a more detailed analysis of neutrino-electron scattering see, for example, S. Godfrey and W. Marciano, in *Proceedings of the Brookhaven National Laboratory Neutrino Workshop*, Upton, New York, 1987, edited by M. J. Murtagh (BNL, Upton, NY, 1987); see also D. London, G. Bélanger, and J. N. Ng, TRIUMF report, 1987 (unpublished).
- ²²W. J. Marciano (private communication).
- ²³Particle Data Group, M. Aguilar-Benitez *et al.*, Phys. Lett. **170B**, 1 (1986).
- ²⁴For a more complete discussion of polarization at the SLC, see *Proposal for Polarization at the SLC*, edited by D. Blockus *et al.*, (SLAC, Stanford, 1986).
- ²⁵B. W. Lynn and C. Verzegnassi, Phys. Rev. D **35**, 3326 (1987).
- ²⁶For more detailed analysis of the effects of extra E_6 neutral gauge bosons in e^+e^- collisions, see, for example, Refs. 7–10, and references therein.
- ²⁷R. Cashmore, Phys. Rep. **122C**, 275 (1985).
- ²⁸E. Eichten, I. Hinchcliffe, K. D. Lane, and C. Quigg, Rev. Mod. Phys. **56**, 579 (1984).
- ²⁹J. Kubar-André and F. E. Paige, Phys. Rev. D **19**, 221 (1979); G. Altarelli, R. K. Ellis, and G. Martinelli, Nucl. Phys. **B143**, 521 (1978); **B146**, 544 (1978).
- ³⁰M. J. Duncan and P. Langacker, University of Pennsylvania Report No. UPR-0293-T (unpublished); V. Barger and W.-Y. Keung, Phys. Rev. D **34**, 2902 (1986); J. L. Hewett and T. G. Rizzo, Ames Laboratory report, 1987 (unpublished).
- ³¹V. Barger and K. Whisnant, Phys. Rev. D **36**, 979 (1987).